Phase diagrams of spin-3/2 Ising model in the presence of random crystal field within the effective field theory based on two approximations

Ali Yigit[a)†] and Erhan Albayrak[b)]

[a)] *Department of Physics, Çankırı Karatekin University*, 18100, *Çankırı*, *Turkey*
[b)] *Department of Physics, Erciyes University*, 38039, *Kayseri*, *Turkey*

(Received 26 March 2013; revised manuscript received 16 April 2013)

The bimodal random crystal field (Δ) effects are investigated on the phase diagrams of spin-3/2 Ising model by using the effective-field theory with correlations based on two approximations: the general van der Waerden identity and the approximated van der Waerden identity. In our approach, the crystal field is either turned on or turned off randomly for a given probability p or $q = 1 - p$, respectively. Then the phase diagrams are constructed on the $(\Delta, kT/J)$ and $(p, kT/J)$ planes for given p and Δ, respectively, when the coordination number is $z = 3$. Furthermore, the effect of randomization of the crystal field is illustrated on the $(\Delta, kT/J)$ plane for $p = 0.5$ when $z = 3, 4$, and 6. All these are carried out for both approximations and then the results are compared to point out the differences. In addition to the lines of second-order phase transitions, the model also exhibits first-order phase transitions and the lines of which terminate at the isolated critical points for high p values.

Keywords: spin-3/2, random crystal field, effective-field theory, isolated critical point

PACS: 05.50.+q, 05.70.Fh, 64.60.Cn, 75.10.Hk **DOI:** 10.1088/1674-1056/22/10/100508

1. Introduction

It is well known that the crystal field (CF) does change the critical behavior of the system drastically, i.e., it may lead to the existence of the first-order phase transitions in the system. If it is strong enough, the energy difference between the split levels is large. In that case, it is energetically more favorable to put as many electrons into the lower energy level before one starts to fill the higher energy level. Filling all the orbitals in the lower level means that one pairs them up (within each orbital) with opposite spins. The effect of pairing electrons with opposite spins makes no addition to the total spin. This results in a low-spin state. Thus its competition with the bilinear interaction parameter leads to first-order phase transitions. In the recent years, the random distribution of CF with some probability, such as the Gaussian, bimodal, trimodal, etc., became popular to investigate. The effect of randomness and distribution type of the CF may change the critical behavior of the system considerably, and therefore, the spin-3/2 Blume–Capel (BC) model with random crystal field (RCF) are studied here by using the effective-field theory (EFT) with correlations.

The effects of CF were studied by using different versions of EFT based on the approximated van der Waerden (AW) identity, for example, the phase diagram and the paramagnetic susceptibility of spin-3/2 were obtained by using the correlated EFT (CEFT).[1] The phase diagrams were obtained for a spin-3/2 Ising model by using a new EFT.[2] The temperature dependencies of the magnetization and the quadrupolar moment in the spin-3/2 Blume–Capel model on honeycomb lattice were examined in detail by the use of a new formulation based on both the exact Ising spin identities and the differential operator technique.[3] The specific heat and magnetic properties of the spin-3/2 transverse Ising model in the presence of CF and anisotropic CF were studied by using the EFT with correlations.[4,5] The ferromagnetisms of the spin-3/2 Ising model with a transverse CF on honeycomb, square, and simple cubic lattices were studied,[6] and the effect of the random external magnetic field in the presence of CF was also studied by using the EFT for the spin-3/2 model.[7,8] On the other hand, the spin-3/2 Ising model was also investigated with EFT based on the general van der Waerden (GW) identity, such as the diluted spin-3/2 Ising ferromagnet on the honeycomb lattice which was investigated by using the EFT with correlations.[9] The specific heat and phase diagrams of the spin-3/2 BC model were obtained by using the same method.[10] The temperature dependencies of the order-parameters of the spin-3/2 BC model on a honeycomb lattice were studied within the framework of an EFT based on the use of the probability distribution.[11] It should be noted that it is the AW that is usually used in the literature when $S \geq 3/2$.

On the other hand, the randomness in the other parameters of the Hamiltonian also does affect the critical behaviors of the model drastically. A few investigations of random bond or random field effects for spin-3/2 by using the EFT include the bond-diluted transverse Ising model in a crystal field on the honeycomb lattice[12] and in a longitudinal random field

†Corresponding author. E-mail: ayigit80@karatekin.edu.tr

© 2013 Chinese Physical Society and IOP Publishing Ltd

with a crystal field[13] and the transverse Ising model in a longitudinal random-field on a honeycomb lattice.[14] The other parameter is the random crystal field which also affects the system considerably. A few examples of this kind are that the random-crystal field spin-1 Blume–Capel model was investigated by the lowest approximation of the cluster-variation method which is identical to the mean-field approximation[15] and in terms of recursion relations on the Bethe lattice[16] and the spin-1 transverse crystal field effects were considered in the EFT and cutting approximation for the spin-1 case.[17] The literature is quite vast for spin-1 models but the spin-3/2 case has not been considered as much.

The RCF effects in the spin-3/2 Ising model were only considered in five research papers as far as we know. The mean-field theory was used in the BC model and thus several new features were obtained including the appearance of a new ordered phase with magnetization $m = 1$ at low temperatures and consequently a rich ground-state phase diagram was calculated.[18] The second work studied the magnetic properties of the bond and CF dilution for the spin-3/2 BC model in an external magnetic field.[19] The third work used the Migdal–Kadanoff renormalization group technique to study the spin-3/2 BC model under an RCF, in the two- and three-dimensional cases and it was found that the randomness removes completely the first order transition between the two ferromagnetic phases presented.[20] The fourth one studied the diluted and symmetric random crystal field in the pair approximation based on Bogoliubov inequality for the free energy and the global phase diagrams were obtained in the temperature versus crystal field plane for the whole range of concentration in the diluted model.[21] Finally, the last work was carried out on the Bethe lattice in which the RCF is turned on with probability p or turned off with probability $1-p$ to obtain the phase diagrams of the BC model.[22] The investigations of RCF effects for the spin-3/2 BC model were investigated in more than these research papers, actually. Thus, in this work we use the EFT with two different approximations to study the RCF effects of the spin-3/2 Ising model. The approach of this study is similar to that of Ref. [22] in a manner such that the CF is either turned on with probability p or turned off with probability $q = 1-p$ randomly in moving on the lattice starting from the central spin to the boundary site spins which are assumed in the $n \to \infty$, i.e., the thermodynamic limit. Thus, the phase diagrams are constructed on the $(\Delta, kT/J)$ and $(p, kT/J)$ planes for given p and Δ, respectively, for the coordination number $z = 3$. The effects of randomization of the CF are also illustrated on the $(\Delta, kT/J)$ plane for $p = 0.5$ for $z = 3, 4$, and 6. We also point out the possible differences of the two approximations AW and GW that are considered here.

The remaining part of this paper is organized as follows. The next section is devoted to the explanation and formulation of our model and the last section includes our illustrations and findings in addition to a brief summary and conclusions.

2. Formulation

The Hamiltonian of spin-3/2 BC model is given as

$$\mathcal{H} = -J \sum_{\langle i,j \rangle} S_i S_j - \sum_i D_i S_i^2, \tag{1}$$

where each S_i located at site i represents a spin-3/2 which takes the discrete values $\pm 3/2$ and $\pm 1/2$; the first sum on the right-hand side runs over all pairs of nearest-neighbor (NN) sites; J is the bilinear interaction parameter between the NN spins; D_i is the site-dependent CF. The latter is distributed in a bimodal fashion according to

$$P(\Delta_i) = p\delta(\Delta_i - \Delta) + (1-p)\delta(\Delta_i), \tag{2}$$

where $\Delta_i = D_i/J$. This random distribution of the CF either turns on or turns off the CF randomly for given probabilities p and $1-p$, respectively, on the sites o thef lattice.

The magnetization of the spin-3/2 Ising model is to be obtained in here by using the EFT with correlations which is a well-known method. This method was first introduced by Honmura and Kaneyoshi[23] and Kaneyoshi *et al.*[24] The order-parameters are obtained in this work by using two identities.

2.1. EFT based on the general van der Waerden identity

The first identity is obtained in the EFT based on the general van der Waerden (GW) identity where the thermal average of a central spin S_i for a lattice with the coordination number z may be written as

$$M = \langle S_i \rangle = \langle \prod_{i=1}^{z} [A(\alpha) + B(\alpha) S_i + C(\alpha)(S_i)^2 + D(\alpha)(S_i)^3] \rangle \times f(x)|_{x=0}, \tag{3}$$

where $\alpha = J\nabla$, with $\nabla = \partial/\partial x$ being the differential operator and the coefficients $A(\alpha)$, $B(\alpha)$, $C(\alpha)$, and $D(\alpha)$ can be calculated by using the van der Waerden identities, see Ref. [2] for example, which are given for spin-3/2 as

$$\begin{aligned} A(\alpha) &= \frac{1}{8}\left[9\cosh\left(\frac{1}{2}\alpha\right) - \cosh\left(\frac{3}{2}\alpha\right)\right], \\ B(\alpha) &= \frac{1}{12}\left[27\sinh\left(\frac{1}{2}\alpha\right) - \sinh\left(\frac{3}{2}\alpha\right)\right], \\ C(\alpha) &= \frac{1}{2}\left[\cosh\left(\frac{3}{2}\alpha\right) - \cosh\left(\frac{1}{2}\alpha\right)\right], \\ D(\alpha) &= \frac{1}{3}\left[\sinh\left(\frac{3}{2}\alpha\right) - 3\sinh\left(\frac{1}{2}\alpha\right)\right]. \end{aligned} \tag{4}$$

Here, $\beta = 1/kT$, with k being the Boltzmann constant, and T being the absolute temperature. The function $f(x)$ in Eq. (3) is defined for spin-3/2 as

$$f(x) = \frac{3\sinh\left(\frac{3}{2}\beta x\right) + \cosh\left(\frac{1}{2}\beta x\right)\exp(-2\beta\Delta_i)}{2\cosh\left(\frac{3}{2}\beta x\right) + 2\cosh\left(\frac{1}{2}\beta x\right)\exp(-2\beta\Delta_i)}. \tag{5}$$

When the term on the right-hand side of Eq. (3) is expanded, the multi-spin correlation functions appear, therefore, the problem becomes much more difficult. In order to ignore these correlations, one can use the decoupling approximation

$$\langle S_i S_{i'} \cdots S_{i^n} \rangle \cong \langle S_i \rangle \langle S_{i'} \rangle \cdots \langle S_{i^n} \rangle \tag{6}$$

for $i \neq i' \neq \ldots \neq i^n$.[25] This approximation corresponds to Zernike approximation in a crystalline Ising ferromagnet.[26] Within the decoupling approximation, equation (3) is obtained by using the GW for $z = 3$ as

$$M = \langle S_i \rangle = [A(\alpha) + B(\alpha)\langle S_i \rangle + C(\alpha)\langle S_i^2 \rangle + D(\alpha)\langle S_i^3 \rangle]^3 \times f(x)|_{x=0}. \tag{7}$$

Expanding the right-hand sides of Eq. (7) and using $\langle (S)^n \rangle = M^n$,[27–29] one can obtain

$$M = a_0 + a_1 M + a_2 M^2 + a_3 M^3 + a_4 M^4 + a_5 M^5 + a_6 M^6 + a_7 M^7 + a_8 M^8 + a_9 M^9, \tag{8}$$

where the coefficients $a_0, a_1, \ldots, a_9$ are not given explicitly here but they are presented in the Appendix A, since they are too long. Here, the quadrupolar order-parameter is not needed, one order-parameter, magnetization, is good enough to analyze the model.

In EFT, the formulation drastically changes as the coordination number changes. Thus the magnetizations for $z = 4$ and 6 can be derived in the same way as it is done for $z = 3$. Thus, it is given for $z = 4$ as

$$M = \langle S_i \rangle = [A(\alpha) + B(\alpha)\langle S_i \rangle + C(\alpha)\langle S_i^2 \rangle + D(\alpha)\langle S_i^3 \rangle]^4 \times f(x)|_{x=0}, \tag{9}$$

with

$$M = \sum_{i=0}^{12} b_i M^i, \tag{10}$$

and for $z = 6$ it is obtained from

$$M = \langle S_i \rangle = [A(\alpha) + B(\alpha)\langle S_i \rangle + C(\alpha)\langle S_i^2 \rangle + D(\alpha)\langle S_i^3 \rangle]^6 \times f(x)|_{x=0}, \tag{11}$$

with

$$M = \sum_{i=0}^{18} c_i M^i. \tag{12}$$

2.2. EFT based on the approximated van der Waerden identity

In the second identity, we again use the EFT, but now based on the approximated van der Waerden (AW) identity. In this case, the order-parameters with the coordination number z may be written as

$$M = \langle S_i \rangle = \langle \prod_{i=1}^{z} [(\cosh(J\eta\nabla) + \frac{S_i}{\eta}\sinh(J\eta\nabla))] \rangle f(x)|_{x=0}, \tag{13}$$

$$\eta^2 = \langle (S_i)^2 \rangle = \langle \prod_{i=1}^{z} [(\cosh(J\eta\nabla) + \frac{S_i}{\eta}\sinh(J\eta\nabla))] \rangle g(x)|_{x=0}, \tag{14}$$

where the approximated van der Waerden identity is given for any spin value as

$$e^{\alpha S_i} = \cosh(\alpha\eta) + \frac{S_i}{\eta}\sinh(\alpha\eta), \tag{15}$$

with

$$\eta^2 = q = \langle (S_i)^2 \rangle. \tag{16}$$

The function $g(x)$ in Eq. (14) is defined for spin-3/2 as

$$g(x) = \frac{9\cosh\left(\frac{3}{2}\beta x\right) + \sinh\left(\frac{1}{2}\beta x\right)\exp(-2\beta\Delta_i)}{4\cosh\left(\frac{3}{2}\beta x\right) + 4\cosh\left(\frac{1}{2}\beta x\right)\exp(-2\beta\Delta_i)}. \tag{17}$$

and the order-parameters are given for $z = 3$ as

$$M = \langle S_i \rangle = \left[(\cosh(J\eta\nabla) + \frac{S_i}{\eta}\sinh(J\eta\nabla)\right]^3 f(x)|_{x=0} \tag{18}$$

and

$$q = \langle (S_i)^2 \rangle = \left[(\cosh(J\eta\nabla) + \frac{S_i}{\eta}\sinh(J\eta\nabla)\right]^3 g(x)|_{x=0}. \tag{19}$$

We again expand terms on the right-hand side of Eqs. (18) and (19) as in the first approximation, then by using the decoupling approximation one can obtain the numerically calculable order-parameter equations. All details of this approximation can be found in Ref. [7].

After obtaining the formulation by using the EFT based on two different approximations, we are now ready to carry out the calculations for the case of the RCF as given in Eq. (2). The calculations are carried out within an iteration scheme (it is the easiest way!) because of the nature of equations for the order-parameters. In the next section, the topological phase diagrams and our findings are presented which are obtained by studying the thermal variations of the magnetizations for given constant values of the other system parameters.

3. Phase diagrams and conclusions

We are now ready to present the phase diagrams of the model. They are obtained in the $(\Delta, kT/J)$ and $(p, kT/J)$ planes for given p and Δ, respectively, when $z = 3, 4$, and 6. The last two coordination numbers are only considered for the effect of randomization of the CF. In the phase diagrams, the second-order phase transition lines, T_c-lines, and the first-order phase transition lines, T_t-lines, are indicated with the solid and dashed lines, respectively. We should note that our main figures are obtained by using GW identity, while the insets are obtained by using AW identity.

Figure 1 illustrates the phase diagrams in the $(\Delta, kT/J)$ plane for given p with the increment of 0.1 when $z = 3$. As seen, the $p = 0$ line corresponds to $\Delta = 0.0$ case for which the T_c-lines are straight lines as expected, since the Hamiltonian has only the interaction parameter J which enters into the formulation as a scaling parameter. When $p = 1$, the model becomes the original spin-3/2 Ising model with constant CF at each site[1–4] which is a well-known and well-studied model. For the intermediate values of p, i.e., for $0 < p < 1$, the model becomes the RCF model. The second-order phase transition lines, i.e., T_c-lines, are seen at higher temperatures at lower p for $\Delta < 0$. While the highest temperature belongs to $p = 0$, the lowest one belongs to $p = 1$. As Δ is increased towards zero, the T_c-lines monotonically increase at lower values of p but the increase is sharper for higher values of p. All the lines intersect at $\Delta = 0$ at the temperature of the $p = 0$ line as expected. The behavior of the T_c-lines are now reversed, that is, they are now seen at higher temperatures for higher p values for $\Delta > 0$. All the lines become constant at some temperatures as $|\Delta|$ becomes very large as seen for each p. Figure 1 of this work is qualitatively very similar to Fig. 2(a) of the Bethe lattice consideration,[22] but the temperatures of the T_c-lines are now somewhat higher. We should mention that the critical lines are seen at higher temperatures for higher z without any qualitative differences, thus, we do not present our results for higher z values. In addition to the T_c-lines, the model also displays the T_t-lines which represent the characteristics of the regular spin-3/2 Ising model. Note that it is really very hard to obtain the first-order lines at low temperatures with the random distribution of Δ. In the main figure, we have only displayed the T_t-line terminating at an isolated critical point obtained for $p = 1.0$, but we know from Ref. [22] that there is a high critical value of p such that the T_t-lines disappear. We see that the phase diagrams are qualitatively similar, but the temperatures of the T_c-lines appear at lower temperatures in the case of AW and there is a T_t-line for $p = 0.9$ in the AW which is not seen in the case of GW. Note also that the AW results are much closer to the results of the Bethe lattice approach.[22] In addition, our results are in agreement with the results of Ref. [20] and in disagreement with those of Ref. [21], i.e., the first-order phase transition lines gradually disappear with the values of p values at higher values decreasing.

Our next phase diagram is calculated in the $(p, kT/J)$ planes for given values of Δ when $z = 3$ which is given in Fig. 2. In the figure, we do not attempt to obtain the T_t lines which are only seen at high p values and at low temperatures as seen in Fig. 1. The straight $\Delta = 0.0$ line again corresponds to the $p = 0$ line of the previous figure. Therefore, all the T_c-lines emerge from the same temperature at $p = 0$ corresponding to the zero CF case. As p increases, the T_c lines are separated and are seen at lower temperatures as Δ becomes more negative, i.e., it decreases, and are seen at higher temperatures as Δ becomes more positive, i.e., it increases. They do not change with the further increase of $|\Delta|$ as seen from the figure for higher negative and positive values of Δ. The T_c-lines obtained for the values of Δ from about -2.0 to higher negative values are combined at the lowest temperature and those for the values of Δ from about 25.0 to higher positive values are combined at the highest temperature when $p = 1$. The T_c-lines between these two cases are terminated at lower temperatures at lower negative values of Δ and at higher temperatures at higher positive values of Δ for $p = 1$. The T_c-lines are again qualitatively similar for different values of z and are seen at higher temperatures for higher z. This figure is again similar to the Fig. 3(a) of Ref. [22], but the temperatures of the T_c-lines are again seen to be higher. Again we see that the temperatures of the T_c-lines in the AW case are lower than those in the GW case. We also see that the T_c-lines start to pile up mutually at about $\Delta \cong 15$ in the AW case and about 25 in the GW case. In addition the T_c-lines at low negative values of Δ are less wiggly in the AW case than those in the GW case.

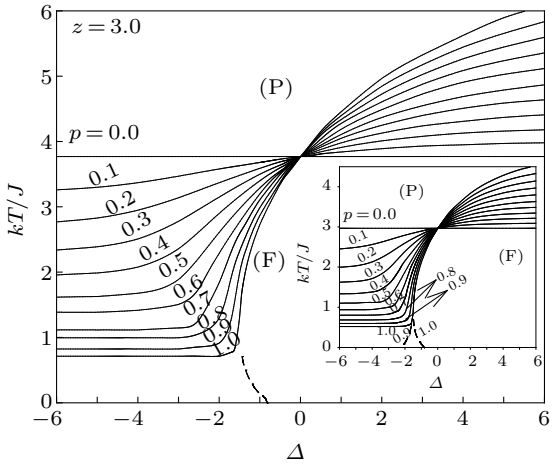


Fig. 1. Phase diagrams in the $(\Delta, kT/J)$ plane for given values of the probability p when $z = 3$ in the GW case and in the AW case in the inset.

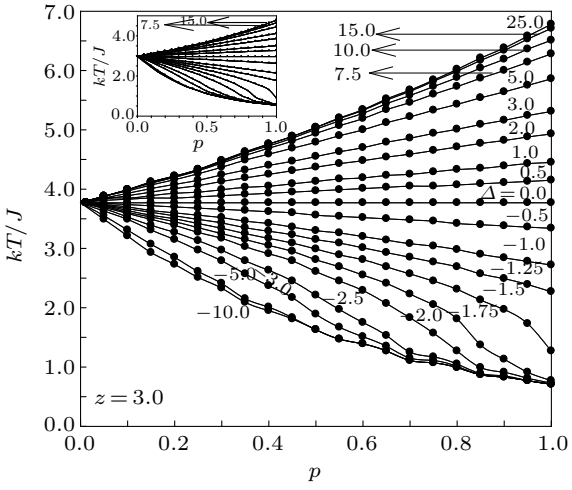


Fig. 2. Phase diagrams in the $(p, kT/J)$ plane for given values of the crystal field Δ when $z = 3$ in the GW case and in the AW case in the inset.

Finally, we investigate the effect of the randomization of the CF on the phase diagram of the model for $p = 0.5$. To do so, we turn on and turn off the CF alternatingly on the sites of the lattice. This alternating distribution of the CF corresponds to a kind of non-random distribution of the crystal field (NRCF). The T_c-lines, i.e., now the gray lines, obtained for the NRCF do not present any changes at high temperatures from the results of the RCF case as shown in Fig. 3. As Δ becomes more negative, the temperatures are lowered and the differences between the RCF and NRCF become much clear even if they are not large. They become more visible at the bending regions of the T_c-lines for each z which is a similar behavior as that in Ref. [22]. This last figure also shows that as z increases the T_c-lines are seen at higher temperatures. The difference between the random case and the non-random case is much more obvious in the AW case and again their temperatures are also lower.

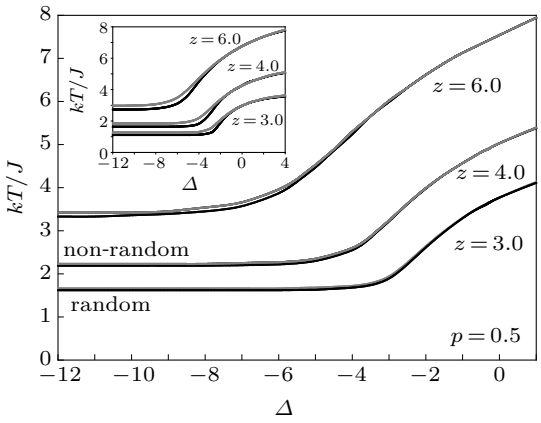


Fig. 3. Phase diagrams in the $(\Delta, kT/J)$ plane for RCF (black lines) and NRCF (gray lines) when $z = 3, 4$, and 6 in the GW case and in the AW case in the inset.

In conclusion, the dependences of the phase diagrams on the bimodal RCF are studied for the spin-3/2 BC model for the coordination numbers $z = 3, 4$, and 6. It is found that the behaviors of the critical lines change drastically with the probability p but the randomness affects their behaviors, which is more obvious in the AW case than in the GW case. Our findings in this work are qualitatively similar to the results of the Bethe lattice work[22] and to the Migdal–Kadonoff renormalization technique results[20] but they are dissimilar to the pair-approximation results.[21] The temperatures of the critical lines are highest in the GW case and they are closer to the Bethe lattice results in the AW case. The existence of the T_tP-line at $p = 0.9$ is consistent with the Bethe lattice result in the AW case but inconsistent in the GW case.

Appendix A

The coefficients, $a_0, a_1, \ldots, a_9$, $b_0, b_1, \ldots, b_{12}$, and $c_0, c_1, \ldots, c_{18}$ in Eqs. (8), (10), and (12), respectively, are easily obtained by using the mathematical relation $\exp(\alpha\nabla)f(x) = f(x+\alpha)$, and they are given as follows:

$$
\begin{aligned}
a_0 = \frac{1}{4096}[&-f(-9J/2) + 27f(-7J/2) - 216f(-5J/2) \\
&+ 240f(-3J/2) + 1998f(-J/2) - f(9J/2) \\
&+ 27f(7J/2) - 216f(5J/2) + 240f(3J/2) \\
&+ 1998f(J/2)],
\end{aligned}
$$

$$\cdots,$$

$$
\begin{aligned}
a_9 = \frac{1}{216}[&-f(-9J/2) + 9f(-7J/2) - 36f(-5J/2) \\
&+ 84f(-3J/2) - 126f(-J/2) + f(9J/2) - 9f(7J/2) \\
&+ 36f(5J/2) - 84f(3J/2) + 126f(J/2)];
\end{aligned}
$$

$$
\begin{aligned}
b_0 = \frac{1}{65536}[&35484f(0) + f(-6J) - 36f(-5J) \\
&+ 450f(-4J) - 1940f(-3J) - 1809f(-2J) \\
&+ 18360f(-J) + f(6J) - 36f(5J) + 450f(4J) \\
&- 1940f(3J) - 1809f(2J) + 18360f(J)],
\end{aligned}
$$

$$\cdots,$$

$$
\begin{aligned}
b_{12} = \frac{1}{1296}[&924f(0) + f(-6J) - 12f(-5J) + 66f(-4J) \\
&- 220f(-3J) + 495f(-2J) - 792f(-J) + f(6J) \\
&- 12f(5J) + 66f(4J) - 220f(3J) + 495f(2J) \\
&- 792f(J)];
\end{aligned}
$$

$$
\begin{aligned}
c_0 = \frac{1}{16777216}[&8193980f(0) + f(-9J) - 54f(-8J) \\
&+ 1161f(-7J) - 12144f(-6J) + 55620f(-5J) \\
&+ 216f(-4J) - 698124f(-3J) + 109296f(-2J) \\
&+ 4835646f(-J) + f(9J) - 54f(8J) + 1161f(7J) \\
&- 12144f(6J) + 55620f(5J) + 216f(4J) \\
&- 698124f(3J) + 109296f(2J) + 4835646f(J)],
\end{aligned}
$$

$$\cdots,$$

$$
\begin{aligned}
c_{18} = \frac{1}{46656}[&(-48620f(0) + f(-9J) - 18f(-8J) \\
&+ 153f(-7J) - 816f(-6J) + 3060f(-5J) \\
&- 8568f(-4J) + 18564f(-3J) - 31824f(-2J) \\
&+ 43758f(-J) + f(9J) - 18f(8J) + 153f(7J) \\
&- 816f(6J) + 3060f(5J) - 8568f(4J) \\
&+ 18564f(3J) - 31824f(2J) + 43758f(J)].
\end{aligned}
$$

References

[1] Gal G L, Kaneyoshi T and Khater A 1993 *Physica A* **195** 174
[2] Kaneyoshi T, Tucker J W and Jaščur M 1992 *Physica A* **186** 495
[3] Kaneyoshi T and Jaščur M 1992 *Physica B* **179** 317
[4] Jiang W, Wei G Z and Xin Z H 2000 *Phys. Stat. Sol. B* **219** 157
[5] Jiang W and Wei G Z 2000 *Physica A* **284** 215
[6] Jiang W, Wei G Z, Du A and Guo L Q 2002 *Physica A* **313** 503
[7] Liang Y Q, Wei G Z, Zhang Q and Xin Z H 2003 *J. Magn. Magn. Mater.* **267** 275
[8] Liang Y Q, Wei G Z, Zhang Q and Xin Z H 2003 *J. Magn. Magn. Mater.* **265** 305
[9] Kaneyoshi T and Jaščur M 1992 *Phys. Stat. Sol. B* **173** K37

[10] Kaneyoshi T and Jaščur M 1992 *Phys. Rev. B* **46** 3374
[11] Peliti L and Saber M 1996 *Phys. Stat. Sol. B* **195** 537
[12] Wei J, Lu Z H , Wei G Z and Du A 2002 *Commun. Theor. Phys.* (Bejing, China) **38** 227
[13] Liang Y Q, Wei G Z, Zhang H and Song G L 2004 *Commun. Theor. Phys.* (Bejing, China) **42** 467
[14] Liang Y Q, Wei G Z and Song G L 2004 *Phys. Stat. Sol. B* **241** 3636
[15] Albayrak E 2013 *Physica A* **392** 552
[16] Albayrak E 2011 *Physica A* **390** 1529
[17] Xu L and Yan S L 2007 *Acta Phys. Sin.* **56** 1691 (in Chinese)
[18] Bahmad L, Benyoussef A and Kenz A El 2008 *J. Magn. Magn. Mater.* **320** 397
[19] Xing L Y and Yan S L 2012 *J. Magn. Magn. Mater.* **324** 3641
[20] Bouziani M E and Gaye A 2013 *Physica A* **392** 2643
[21] Peña Lara D and Plascak J A 1998 *Physica A* **260** 443
[22] Albayrak E 2011 *J. Magn. Magn. Mater.* **323** 2846
[23] Honmura R and Kaneyoshi T 1979 *J. Phys. C: Solid State Phys.* **12** 3979
[24] Kaneyoshi T, Fittipaldi I P, Honmura R and Manabe T 1981 *Phys. Rev. B* **24** 481
[25] Tamura I and Kaneyoshi T 1981 *Prog. Theor. Phys.* **66** 1892
[26] Zernike F 1940 *Physica* (Utrecht) **7** 565
[27] Ertas M, Deviren B and Keskin M 2012 *J. Magn. Magn. Mater.* **324** 704
[28] Deviren B and Keskin M 2012 *J. Magn. Magn. Mater.* **324** 1051
[29] Ertas M, Keskin M and Deviren B 2012 *J. Magn. Magn. Mater.* **324** 1503